

A study of the core of the Shapley Concentration: III. Properties of the clusters in the A3558 complex [★]

S. Bardelli¹, E. Zucca^{2,3}, G. Zamorani^{2,3}, G. Vettolani³ & R. Scaramella⁴

¹ *Osservatorio Astronomico di Trieste, via Tiepolo 11, I-34131 Trieste, Italy*

² *Osservatorio Astronomico di Bologna, via Zamboni 33, I-40126 Bologna, Italy*

³ *Istituto di Radioastronomia del CNR, via Gobetti 101, I-40129 Bologna, Italy*

⁴ *Osservatorio Astronomico di Roma, via Osservatorio 2, I-00040 Monteporzio Catone (RM), Italy*

E-mail: bardelli@astrts.oat.ts.astro.it

Received 00 - 00 - 0000; accepted 00 - 00 - 0000

ABSTRACT

The Shapley Concentration is the richest supercluster of clusters in the nearby universe and its core is a remarkable complex formed by the ACO clusters A3558, A3562 and A3556, and by the two minor groups SC 1327-312 and SC 1329-314. This structure has been studied in various wavelength bands, revealing that it is probably dynamically very active. In this paper we present 174 new galaxy redshifts in this cluster complex, which are added to the sample of 540 already existing velocities. The large number of redshifts permits a more accurate and robust analysis of the dynamical parameters of the clusters. In particular, we discuss the complex velocity distribution of A3558, the bimodal distribution of A3556 and SC 1329-313, and calculate the mean velocity and velocity dispersion of A3562. Moreover, for the three ACO clusters we derive the luminosity functions adopting a new fitting technique, which takes into account the galaxy density profiles.

Key words: galaxies– clusters– individuals: A3558– A3562– A3556– SC 1329-313– SC 1327-312– SC 1329-314

1 INTRODUCTION

The Shapley Concentration supercluster, at a distance of $\sim 140 \text{ h}^{-1} \text{ Mpc}$ ($h=H_0/100$), is a very interesting region, which makes possible the detailed study of the formation and evolution of clusters of galaxies and of the role played by the environment on these phenomena. The high local density contrast, as traced by the distribution of Abell–ACO clusters (Scaramella et al. 1989; Zucca et al. 1993), X–ray clusters (Lahav et al. 1989) and both optical (Raychaudhury et al. 1991) and IRAS galaxies (Allen et al. 1990), suggests the presence of high peculiar velocities of the order of $\sim 1000 \text{ km/s}$ (Branchini & Plionis 1996). This fact, added to the richness in clusters of this supercluster (it is the richest one within $300 \text{ h}^{-1} \text{ Mpc}$, Zucca et al. 1993), leads to an increase of the cross–section for interactions, like cluster–cluster and group–cluster mergings. Raychaudhury et al. (1991), noting that the percentage of multiple nuclei clusters is much higher than in the field, suggested a merging rate between 1.5 and 3 times higher than elsewhere.

The core of the Shapley Concentration is individuated

by a remarkable chain formed by the three ACO (Abell et al. 1989) clusters A3556, A3558 and A3562, already noted by Shapley (1930). This complex is an aligned structure, elongated $\sim 3^\circ$ in the East–West direction, with a comoving size of $\sim 7.5 \text{ h}^{-1} \text{ Mpc}$. As noted by Metcalfe et al. (1994), A3556 (richness class 0) and A3562 (richness class 2) lie within the Hubble turnaround radius of A3558, and probably they are going to merge with the latter.

The bi–dimensional distribution of galaxies suggests that these clusters are strongly interacting and are forming a single connected structure (Bardelli et al. 1994, hereafter Paper I; Metcalfe et al. 1994). In particular, it is possible to individuate a number of secondary subclumps surrounding A3558 (see Figure 14 of Paper I), revealing the complex dynamical state of this structure.

In Paper I we presented the results of an extensive spectroscopic survey in this area, using a sample of ~ 300 new redshifts, to be added to the 200 from literature (Metcalfe et al. 1987; Teague et al. 1990). We confirmed that the three ACO clusters are at the same distance and are aligned in a filament approximately perpendicular to the line of sight. Moreover we studied two subcondensations between A3558 and A3562, near the position of the poor cluster SC 1329–314; the reality of these groups was confirmed by observa-

[★] based on observations collected at the European Southern Observatory, La Silla, Chile.

tions in the X-ray band by Bardelli et al. (1996, hereafter Paper II) and Breen et al. (1994), who detected extended emission from the hot gas trapped in their gravitational wells. A significant X-ray emission connecting A3558 with the nearest group (dubbed SC 1327–312 by Breen et al.) has been detected (see Paper II), confirming the presence of strong gravitational interactions between these components. This fact reinforces the suggestion by Metcalfe et al. (1994) that there was already an encounter between A3562, A3558 and the two groups. These collisions, expected in a hierarchical scenario of formation of cosmic structures, have been studied through numerical simulations by McGlynn & Fabian (1984) and Roettiger et al. (1993) and have probably been observed in A2256 (Briel et al. 1991) and Coma (Burns et al. 1994).

Moreover, the merging between a cluster and a group could explain the formation of the central dominant galaxies. Indeed, following Tremaine (1990), such galaxies are likely to form in low velocity dispersion systems (such as groups), which are then captured by clusters and deposited at their centers through dynamical friction.

For these reasons the detailed study of interacting clusters, and in particular of their dynamical state, is important: this can be done with the simultaneous use of bi-dimensional and velocity information. Therefore it is necessary to cover wide areas with multifiber spectroscopy, in order to obtain large redshift samples, which are necessary to study all the details of the galaxy distribution.

In this paper we present various properties (dynamical parameters, luminosity functions, density profiles) of the clusters in the A3558 complex, using also ~ 200 new galaxy redshifts. The paper is organized as follows: in Sect.2 we present the galaxy sample and in Sect.3 we describe the analyses applied to the clusters; the results for each cluster are given in Sect.4 and finally in Sect.5 there is the summary.

2 THE SAMPLE

2.1 The galaxy catalogue

Figure 1a shows the isodensity contours for the objects with $b_J \leq 19.5$ from the COSMOS/UKST galaxy catalogue (Yentis et al. 1992), in a region of $3^\circ.2 \times 1^\circ.4$, corresponding to $13^h 22^m 06^s < \alpha(2000) < 13^h 37^m 15^s$ and $-32^\circ 22' 40'' < \delta(2000) < -30^\circ 59' 30''$. This region is part of the UKSTJ plate 444 and contains 2241 galaxies within the chosen limits. The radius of the dashed circles, centered on A3562, A3558 and A3556, corresponds to 1 Abell radius ($\sim 1.5 \text{ h}^{-1} \text{ Mpc}$); the overdensity between A3562 and A3558 corresponds to SC 1329–314. Figure 1b shows, superimposed on the galaxy contours, the position of the fields observed with the multifiber spectrograph OPTOPUS (solid circles with 32 arcmin diameter): the five numbered fields correspond to the new observations, while the others refer to the data reported in Paper I. Field 1, which corresponds to the center of A3562, was observed twice in order to compensate the completely failed previous observations, and field 2 is a further observation of the center of A3556, previously observed as field 9 (see Paper I).

The coordinates and the observation dates of the new fields are reported in Table 1.

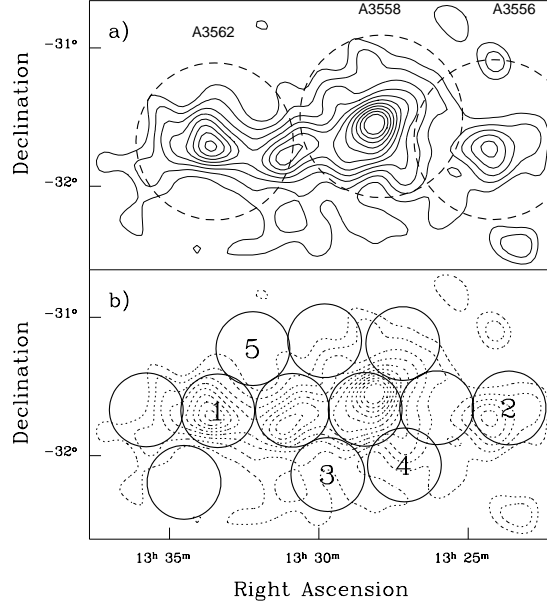


Figure 1. a) Isodensity contours of the core of the Shapley Concentration in an area of $\sim 3^\circ.2 \times 1^\circ.4$. The figure refers to galaxies with $b_J \leq 19.5$ and binned in $2 \times 2 \text{ arcmin}^2$ bins; the data have been smoothed with a Gaussian with a FWHM of 6 arcmin. For the three Abell clusters circles of one Abell radius have been drawn (dashed curves); the poor cluster SC 1329–314 is the peak between the clusters A3558 and A3562. b) The same as in panel a), with superimposed the observed OPTOPUS fields: circles with numbers refer to the new observations, the others correspond to the sample of Paper I.

Table 1. Centers of the observed fields

Field	α (2000)	δ (2000)	Observation date
1	13 33 30	-31 40 00	21 Feb 1993
2	13 23 36	-31 39 21	21 Feb 1993
3	13 29 45	-32 07 43	22 Feb 1993
4	13 27 15	-32 05 00	24 Feb 1993
5	13 32 15	-31 12 17	23 Feb 1993

2.2 Observations and data reduction

The spectroscopic observations were performed at the 3.6m ESO telescope at La Silla, equipped with the OPTOPUS multifiber spectrograph (Lund 1986), on the nights of 21–22–23–24 February 1993. The OPTOPUS multifiber spectrograph uses bundles of 50 optical fibers, which can be set within the field of the Cassegrain focal plane of the telescope; this field has a diameter of 32 arcmin, and each fiber has a projected size on the sky of $\sim 2.5 \text{ arcsec}$. We used the ESO grating # 15 (300 lines/mm and blaze angle of $4^\circ 18'$) allowing a dispersion of 174 \AA/mm (corresponding to a resolution of $\sim 12 \text{ \AA}$) in the wavelength range from 3700 to 6024 \AA . The detector was the Tektronix 512 \times 512 CB CCD (ESO #32) with a pixel size of $27 \mu\text{m}$, corresponding to 4.5 \AA , i.e. a velocity bin of $\sim 270 \text{ km/s}$ at 5000 \AA . This detector has a good responsive quantum function in the blue ($\sim 70\%$

at 4000 Å), where there are the calcium and [OII] lines. Following Wyse & Gilmore (1992), we dedicated 5 fibers to sky measurements, remaining with 45 fibers available for the objects. The observing time for each field was one hour, split into two half-hour exposures in order to minimize the effects due to the “cosmic” hits. The observing sequence was: a 30 seconds exposure of a quartz–halogen white lamp, a 180 seconds exposure of the Phillips Helium and Neon arcs, then the first and the second field exposures, and again the arcs and the white lamp.

The reduction steps are described in Paper I. However, it could be important to stress that we normalized the fiber transmission dividing each spectrum by the continuum–subtracted flux of the sky emission line [OII]λ 5577. This procedure assumes that the sky emission does not change significantly on angular scales of the order of ~ 30 arcmin (Wyse & Gilmore 1992).

We obtained estimates of the radial velocity of galaxies using the cross–correlation method as implemented in the IRAF[†] task RVSAO (XCSAO, Kurtz et al. 1992). The galaxy spectra were cross–correlated with those of 8 stellar templates observed with the same instrumental set up. The adopted velocity for each galaxy is the value given by the template which gives the minimum cross–correlation error. For spectra with strong emission lines we measured an “emission velocity” using the EMSAO program in the same IRAF task RVSAO.

2.3 The new redshift data

From the total number of spectra (266), it was possible to obtain 214 velocity estimates: 40 objects turned out to be stars ($\sim 19\%$ of the reliable spectra), leaving us with 174 new galaxy redshifts. The high number of failed spectra ($\sim 19\%$ of the total number of spectra) is mainly due to technical problems in the second exposure (fainter galaxies) of field #1: if we do not consider this exposure, the total number of spectra is 222 with 19 failed spectra ($\sim 9\%$).

In Table 2 we list the objects with velocity determination. Column (1) is the sequential number, columns (2), (3) and (4) give the right ascension (2000), the declination (2000) and the b_J apparent magnitude, respectively, as reported in the COSMOS catalogue. Columns (5) and (6) give the heliocentric velocity ($v = cz$) and the internal error (in km/s); the word “star” in column (5) indicates those objects which turned out to be stars after the spectral analysis. The external error can be derived by multiplying the error in column (6) by a factor of the order of 1.6 – 1.9: the lower value is obtained by comparing repeated observations of the same galaxies (Malumuth et al. 1992) and the higher one takes into account also the different reduction techniques (see the discussion in Paper I). Finally, the code “emiss” in column (7) denotes the velocities determined from emission lines.

The galaxies whose spectrum presents detectable emission lines (mainly [OII]λ 3727, Hβ λ 4860, [OIII]λ 4959 and [OIII]λ 5007) are 30, corresponding to a percentage of 17%, in agreement with the average value of 16% reported by Biviano et al. (1997a, 1997b) for the cluster galaxy population.

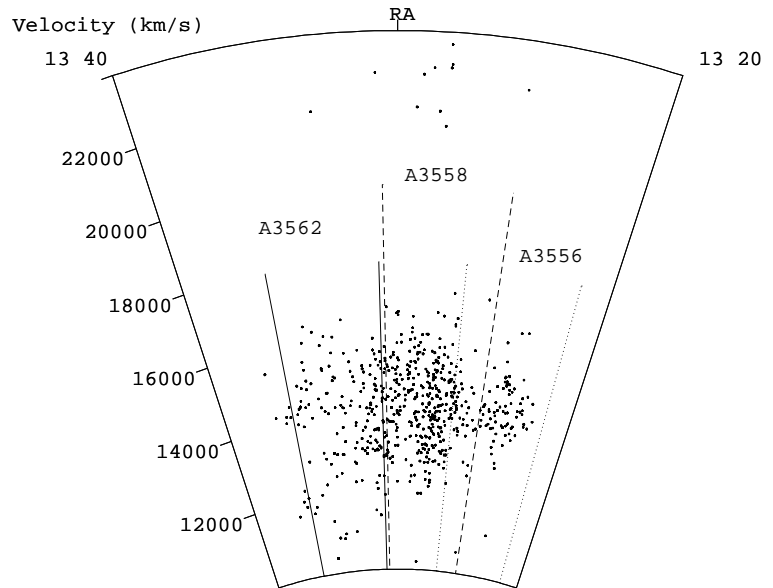


Figure 2. Wedge diagram of the sample of galaxies in the velocity range 10000 – 24000 km/s. The coordinate range is $13^{\text{h}}22^{\text{m}}06^{\text{s}} < \alpha(2000) < 13^{\text{h}}37^{\text{m}}15^{\text{s}}$ and $-32^{\circ}22'40'' < \delta(2000) < -30^{\circ}59'30''$. The three pairs of straight lines (solid, dashed and dotted) show the projection in right ascension of 1 Abell radius for the three clusters A3562, A3558 and A3556, respectively.

Adding also the previous data, the total spectroscopic sample consists of 714 galaxy redshifts: 511 are those used in Paper I, 29 are from Quintana et al. (1995) and 174 are our new determinations. The completeness of the spectroscopic survey at $b_J \leq 19.5$ is $\sim 31\%$ ($\sim 50\%$ at $b_J \leq 18.0$) in the entire area, but it strongly varies with the position: within one Abell radius from the cluster centers we have $\sim 45\%$ of the redshifts for A3558 ($\sim 82\%$ at $b_J \leq 18.0$), $\sim 26\%$ ($\sim 55\%$) for A3562 and $\sim 30\%$ ($\sim 68\%$) for A3556.

In Figure 2 we show the wedge diagram of this sample in the velocity range [10000 – 24000] km/s. This wedge, with $\sim 40\%$ more redshifts than those presented in Paper I, confirms the connection between the clusters: the A3558 complex is a single structure of galaxies, ranging from A3556 to A3562. In particular, the data now available for A3562 permits to study also the eastern part of the complex, where the galaxy distribution appears to be less concentrated and the existence of a “finger-of-God” effect is not clear.

In Figure 3 the velocity distribution of the 174 new redshifts (shadowed histogram) is shown, superimposed to the data used in Paper I. It is clear that both samples well represent the overdensity at the distance of the core of the Shapley Concentration (~ 15000 km/s) and the void (at ~ 20000 km/s), already noted in Paper I, just behind the structure.

3 ANALYSIS OF THE CLUSTERS

[†] IRAF is distributed by KPNO, NOAO, operated by the AURA, Inc., for the National Science Foundation.

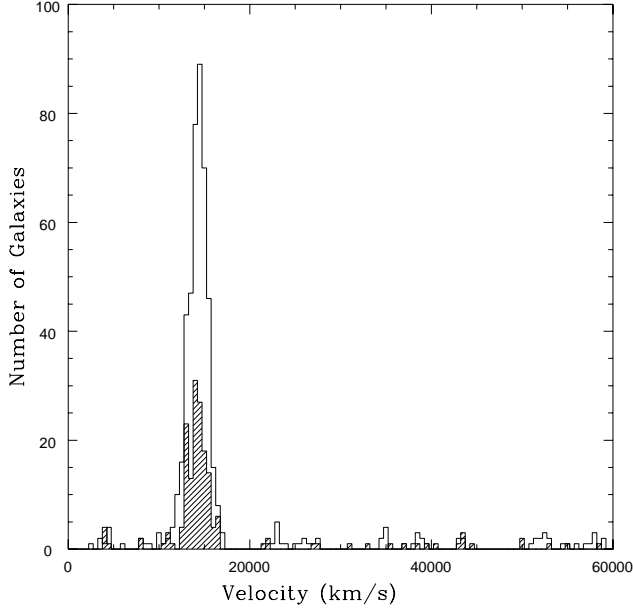


Figure 3. Velocity distribution for the 174 new redshifts (shaded histogram), superimposed to the data used in Paper I (open histogram). It is clear the presence of the overdensity corresponding to the core of the Shapley Concentration (at ~ 15000 km/s) and a void at ~ 20000 km/s, well represented in both samples.

3.1 Dynamical parameters

In order to estimate the dynamical parameters of the cluster velocity distribution, i.e. the mean velocity $\langle v \rangle$ and the velocity dispersion σ , we used the biweight location and scale estimators, respectively (see Beers et al. 1990 for their definitions). The advantage of these estimators, with respect to the standard mean and dispersion, is that of minimizing biases from interlopers, giving less weight to data with higher distance from the median. The derived velocity dispersions are then corrected for the broadening due to velocity errors, following Danese et al. (1980). The confidence intervals of the two estimators are calculated bootstrapping the data with 100 random catalogs.

In order to find the velocity range in which the cluster members lie, we have assumed that the velocity distribution of cluster galaxies is Gaussian, as expected when the system has undergone a violent relaxation (see details in Paper I). For the cases in which the presence of a substructure was suspected on the basis of either the shape estimators a , b_1 , b_2 and I (see Bird & Beers 1993) or a visual inspection of the velocity histogram, we checked if the distribution is consistent with a single Gaussian or it is bimodal applying the KMM test (Ashman et al. 1994), using the program kindly provided by the authors. This test gives the likelihood ratio between the hypothesis that the dataset is better described by the sum of two Gaussians and the null hypothesis that the dataset is better described by a single Gaussian. The value of the likelihood ratio, as computed by the program, is a rigorous estimate of the confidence limit of the null hypothesis only when testing the existence of two Gaussians with equal dispersions (homoscedastic distributions), but can be taken as a reasonable approximation also in the case of dif-

Table 3. Dynamical parameters of the clusters

Name	$\langle v \rangle$ (km/s)	σ (km/s)	N_{gal}	notes
A3556	14357^{+76}_{-76}	643^{+53}_{-43}	79	$r < 22$ arcmin
	14130^{+42}_{-74}	411^{+76}_{-29}	56	substr. 1
	15066^{+58}_{-43}	222^{+59}_{-35}	23	substr. 2
A3558	14403^{+60}_{-55}	996^{+40}_{-36}	307	$r < 1 r_{Abell}$
	14262^{+75}_{-82}	992^{+85}_{-60}	155	$r < 0.5 r_{Abell}$
	14260^{+100}_{-67}	946^{+70}_{-80}	117	$b_J > 17$
	14309^{+285}_{-219}	1125^{+139}_{-79}	31	$b_J < 17$
	12993^{+129}_{-119}	310^{+119}_{-92}	11	$b_J < 17$ substr. 1
	14871^{+144}_{-145}	455^{+51}_{-55}	20	$b_J < 17$ substr. 2
SC 1329–313	14790^{+114}_{-67}	377^{+93}_{-82}	16	substr. 1
	13348^{+69}_{-83}	276^{+70}_{-61}	21	substr. 2
SC 1327–312	14844^{+105}_{-211}	691^{+158}_{-146}	24	
A3562	14492^{+225}_{-286}	913^{+189}_{-96}	21	$r < 10$ arcmin

ferent dispersions (heteroscedastic) (Ashman et al. 1994). However, in the cases in which we found bimodality in our data, the bimodal distribution was significant both in the homoscedastic and in the heteroscedastic case (if not otherwise specified).

In the case of bimodality, the KMM program gives for each galaxy the “a posteriori probability” of the group membership: after having divided the two groups on this basis, we have repeated the estimate of mean velocity and velocity dispersion for each of them following the previous criteria.

The results of the dynamical analysis of the considered clusters are reported in Table 3. The first column lists the cluster name, the second and third columns give the mean velocity and velocity dispersion, the fourth column reports the number of galaxies used for the determination of the parameters and in the fifth column there are the characteristics of the used samples. The discussion of the results for each cluster is reported in Sect.4.

3.2 Luminosity functions

In order to estimate the cluster luminosity function it is necessary to correct the number of galaxies for the foreground and background contamination. In general this is done assuming a universal number–counts relation, as done for example by Colless (1989) for a sample of 14 rich clusters and by Metcalfe et al. (1994) for A3558. This approach is not correct for our clusters, because of the existence of the underlying supercluster, the presence of the Great Attractor overdensity at ~ 4000 km/s and of other structures behind the Shapley Concentration (see Bardelli et al. 1997) in approximately the same direction of the A3558 complex: therefore we chose to estimate a local background, extracting counts from regions without obvious overdensities in the same UKSTJ plate which contains the A3558 complex (#444), obtaining a total control area of ~ 10 square degrees. Comparing these counts with those obtained from a reference region of ~ 140 square degrees toward the South Galactic Pole (from the Edinburgh–Durham Southern Galaxy Catalogue, Heydon–Dumbleton et al. 1989) we found, as expected, that

they present an excess at all magnitudes. Such an excess corresponds to an average factor of ~ 1.5 at $17.5 < b_J < 19.5$.

Assuming that the luminosity function is well described by a Schechter (1976) form

$$\phi(L)dL = \phi^* \left(\frac{L}{L^*}\right)^\alpha e^{-L/L^*} d\left(\frac{L}{L^*}\right) \quad (1)$$

the probability of seeing a galaxy with $L_i > L_{min}$ is

$$p_i = \left(\frac{\phi(L_i)}{\int_{L_{min}}^{\infty} \phi(L_i)}\right)^{w_i} \quad (2)$$

where L_{min} is the minimum absolute luminosity corresponding to the limiting apparent magnitude of our survey ($b_J = 19.5$) at the distance of each cluster. The term w_i is a weight which takes into account the background correction and corresponds to the probability that the i^{th} galaxy in the photometric sample belongs to the cluster. In general, w_i is a function of both magnitude m and distance r from the cluster center and can be computed as

$$w_i(m, r) = \frac{N_{cl}(m, r)}{N_{tot}(m, r)} = \frac{[N_{tot}(m) - N_{bck}(m)]f(r)dr}{[N_{tot}(m) - N_{bck}(m)]f(r)dr + N_{bck}(m)\frac{2\pi r}{\pi r_{max}^2}dr} \quad (3)$$

where N_{tot} is the number of galaxies in the projected cluster region and N_{bck} is the number of ‘‘background’’ galaxies expected in the same region (from the estimate in the control area) and $N_{cl} = N_{tot} - N_{bck}$. The function $f(r)$ represents the ratio

$$f(r) = \frac{2\pi r I(r)}{\int_0^{r_{max}} 2\pi r I(r) dr} \quad (4)$$

where $I(r)$ is the surface density of galaxies (see next Section) and r_{max} is the maximum distance from the cluster center.

If we neglect the radial dependence, as usually done in the literature, eq.(3) reduces to

$$w_i = 1 - \frac{N_{bck}(m)}{N_{tot}(m)} \quad (5)$$

The numbers N_{bck} and N_{tot} were computed in bins of 0.2 magnitudes, for both eq.(3) and eq.(5). The parameters reported in the following were derived using eq.(3): however the parameters obtained with eq.(5) are always consistent with them within 1σ errors.

The parameters of the fitting function are derived through a maximum likelihood technique, minimizing the product of the p_i taking into account the weights. This method is the same as that applied by Zucca et al. (1994), estimating the luminosity function when the sample is affected by incompleteness. In the incompleteness case, the weights are greater than one in order to correct for the objects missed or not observed in a given magnitude bin. On the contrary, in our case the weights are smaller than one because, due to the presence of the background contamination, the sample used to compute the luminosity function (i.e. the photometric catalogue) contains also objects which do not belong to the clusters.

Very recently, Lumsden et al. (1997) found that the COSMOS magnitude scale is not linear for bright objects

Table 4. Parameters of the cluster luminosity functions

Name	α	M^*	notes
A3556	$-1.10^{+0.32}_{-0.29}$	$-19.14^{+0.50}_{-0.73}$	$b_J > 15.5$
A3558	$-1.39^{+0.12}_{-0.12}$	$-20.26^{+0.39}_{-0.56}$	$b_J > 15.0$
A3562	$-1.42^{+0.19}_{-0.15}$	$-19.84^{+0.46}_{-0.61}$	$b_J > 15.0$

($b_J \lesssim 17$), because of a lack of dynamic range of the measuring machine, and proposed a correction for $15 < b_J < 21$ based on the comparison with CCD photometry. The corrected magnitudes are brighter than the original ones and this effect is at maximum ~ 0.45 mag at $b_J = 15$. Therefore, when fitting the cluster luminosity functions, we adopted this correction and we considered only galaxies with $b_J > 15$.

Finally, the correction for galactic absorption has been applied using the extinction values reported by Burstein & Heiles (1984): the values are $A_B = 0.181$, $A_B = 0.169$ and $A_B = 0.189$ in the direction of the center of A3558, A3562 and A3556, respectively.

The best fit parameters (with 1σ errors) of the Schechter form of the luminosity function of these three clusters are reported in Table 4 (cluster name in column 1, α and M^* in column 2 and 3); the discussion of the results is presented in Sect.4.

The parameters M^* presented in the following have been derived including the Lumsden et al. and the galactic absorption corrections, adopting a distance modulus of $35.79 - 5 \log h$. On the contrary, when speaking about apparent magnitudes we always refer to the original (i.e. without corrections) COSMOS magnitudes.

3.3 Density profiles

For the fit of the radial density galaxy profiles, we assume a King law of the form

$$I(r) = I_o \left(1 + \left(\frac{r}{r_c}\right)^2\right)^{-\alpha} \quad (6)$$

where $I(r)$ is the surface density of galaxies (in $\text{h}^2 \text{Mpc}^{-2}$ or arcmin^{-2}) at distance r from the cluster center, r_c is the core radius (in $\text{h}^{-1} \text{Mpc}$ or arcmin), α is the profile steepness (generally fixed to one) and I_o is the normalization (in $\text{h}^2 \text{Mpc}^{-2}$ or arcmin^{-2}). We minimize the likelihood function

$$\mathcal{L} = \prod_1^{N_{gal}} \frac{2\pi r_i [I(r_i) + bck]}{\int_0^{r_{max}} 2\pi r [I(r) + bck] dr} \quad (7)$$

where bck is the background ($\text{h}^2 \text{Mpc}^{-2}$ or arcmin^{-2}), r_i ($\text{h}^{-1} \text{Mpc}$ or arcmin) is the radial distance of the i^{th} galaxy from the cluster center and r_{max} is the maximum radial extension of the sample.

The results for A3556, A3558 and A3562 are reported in Table 5: column 1 lists the cluster name, column 2 gives α , in column 3 there is r_c (in arcmin), and columns 4 and 5 report I_o and bck (in arcmin^{-2}), respectively. The discussion of the various cases is presented in Sect.4.

Assuming spherical symmetry and that the orbits are isotropic and the velocity dispersion is not a function of the

Table 5. Parameters of the radial density profiles

Name	α	r_c (arcmin)	I_0 (arcmin $^{-2}$)	bck (arcmin $^{-2}$)	notes
A3556	0.55	0.90	0.45	0.01	$b_J \leq 18$
A3558	0.85	3.60	0.90	0.15	
A3562	0.70	3.10	0.70	0.10	

distance from the cluster center (i.e. the cluster is isothermal), it is possible to have an estimate of the total mass inside the radius r using the formula (Binney & Tremaine 1987)

$$M(< r) = -\frac{r\sigma^2}{G} \frac{d \ln \rho}{d \ln r} \quad (8)$$

where ρ is the spatial (i.e. tri-dimensional) distribution of galaxies, σ the velocity dispersion of the cluster and $M(< r)$ is the total mass inside the radius r . Note that the hypothesis that the cluster is isothermal is supported (at least for A3558) by the fact that the distributions of both hot gas temperature (see Paper II) and observed velocity dispersion (see Paper I) do not strongly vary with the distance from the cluster center.

The spatial distribution ρ is derived from the galaxy surface density distribution, through the standard Abel inversion, and it results

$$\rho = \rho_o \left(1 + \left(\frac{r}{r_c}\right)^2\right)^{-\alpha-0.5} \quad (9)$$

where ρ_o is the central density (see The & White 1986).

4 RESULTS

4.1 A3556

A3556 is a poor cluster (richness class 0), classified in the Bautz–Morgan class I, although it is dominated by two giant ellipticals with $b_J = 14.32$ and $b_J = 14.49$ at $v = 14074$ km/s and $v = 14459$ km/s, respectively.

Previous determinations of the dynamical parameters are from Paper I ($\langle v \rangle = 14407 \pm 89$ km/s, $\sigma = 554 \pm 47$ km/s, using 48 galaxies), from Quintana et al. (1995; $\langle v \rangle = 14167 \pm 116$ km/s, $\sigma = 538_{-64}^{+98}$ km/s, based on 25 galaxies) and Stein (1997; $\langle v \rangle = 14574 \pm 86$ km/s, $\sigma = 459 \pm 44$ km/s, based on 30 galaxies). From these values it is clear that, although the velocity dispersion determinations are in agreement, the mean velocity estimates are not consistent within the quoted errors: the reason of this inconsistency is clarified using our new sample.

The angular separation between the centers of A3556 and A3558 is only ~ 50 arcmin, while the Abell radius at the distance of the clusters is ~ 36 arcmin. Therefore, if the angular extension of the velocity sample around the cluster center is comparable with these sizes, the contamination by objects from the nearby cluster could be important. For this reason, we decided to consider only objects within 22 arcmin from the cluster center in the analysis of the dynamical parameters: this value was chosen on the basis of

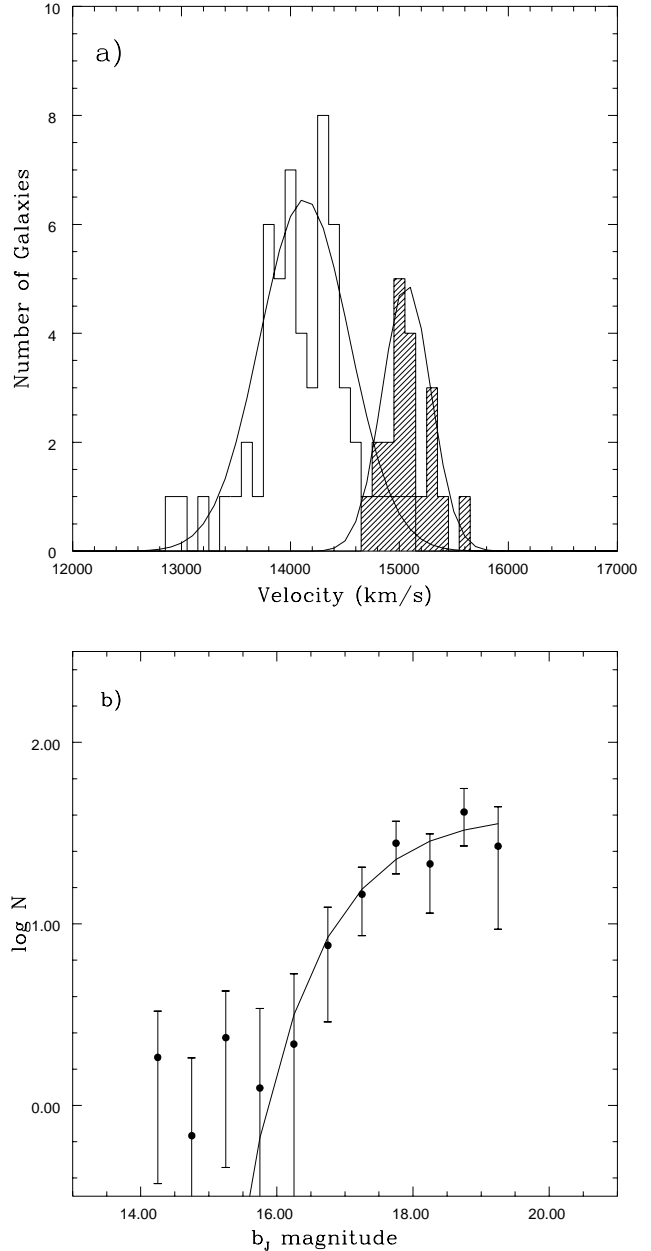


Figure 4. a) Redshift distribution for the galaxies within 22 arcmin from the center of A3556, divided in the two components. Open histogram corresponds to the members of a group with $\langle v \rangle = 14130_{-74}^{+42}$ km/s and $\sigma = 411_{-29}^{+76}$ km/s, while shadowed histogram corresponds to members of a group with $\langle v \rangle = 15066_{-43}^{+58}$ km/s and $\sigma = 222_{-59}^{+35}$ km/s. b) Luminosity function of A3556. The fitted parameters are $\alpha = -1.10_{-0.29}^{+0.32}$ and $M^* = -19.14_{-0.73}^{+0.50}$, after having excluded the objects brighter than $b_J = 15.5$.

a visual inspection of both the isodensity contours and the wedge diagram.

Using the new sample, the estimated parameters on the basis of 79 velocities are $\langle v \rangle = 14357_{-76}^{+76}$ km/s and $\sigma = 643_{-43}^{+53}$ km/s. However, from the redshift histogram shown in Figure 4a, it is clear that the distribution presents two distinct peaks: applying the KMM test we found that

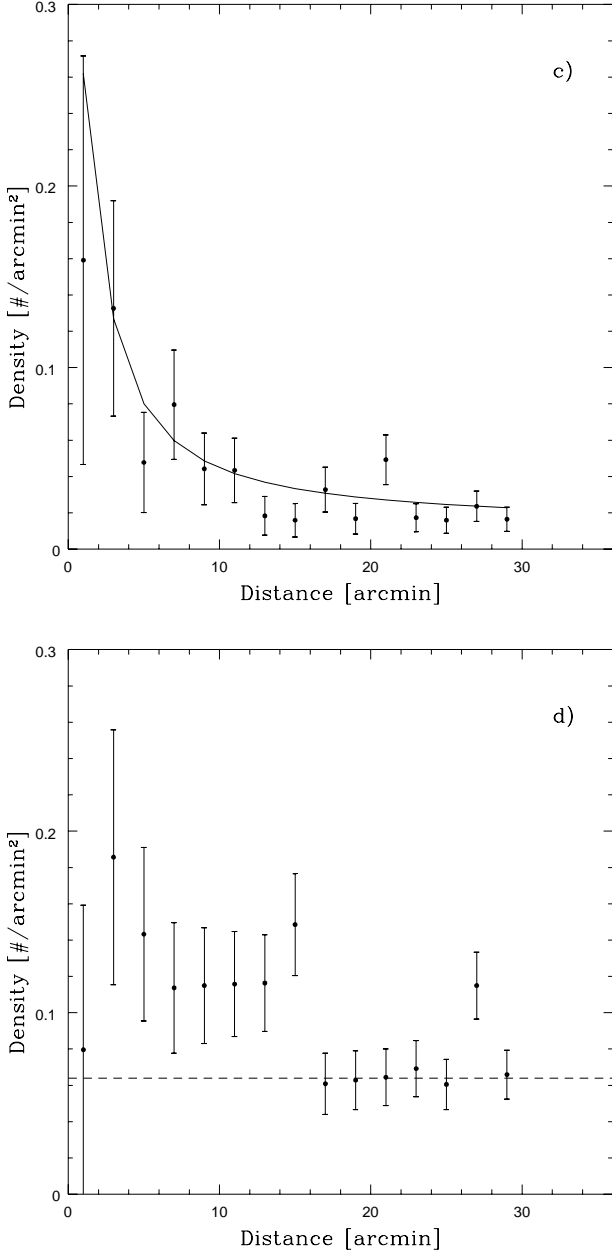


Figure 4. c) Galaxy density distribution in A3556, as a function of the distance from the cluster center; only galaxies with $b_J \leq 18$ are considered. No background subtraction has been applied in this figure.

d) Same as panel c), but considering objects with $18 < b_J \leq 19.5$. The dashed line represents the background as estimated in the control area in the same magnitude range.

the heteroscedastic bimodality is significant and the single Gaussian distribution is rejected at a confidence level of 97.5%. The biweight estimators of the position and the scale for the two distributions are $\langle v \rangle_1 = 14130_{-74}^{+42}$ km/s, $\sigma_1 = 411_{-29}^{+76}$ km/s and $\langle v \rangle_2 = 15066_{-43}^{+58}$ km/s, $\sigma_2 = 222_{-35}^{+59}$ respectively. The number of objects assigned to the two peaks is 56 to the lower velocity clump and 23 to the other one. Note that the mean velocity determination of Quintana et al. (1995) is well consistent with the first substructure:

given the limited number of redshifts used by these authors (25), their sample could be dominated by this clump. A KS analysis of the velocity distribution between bright ($b_J \leq 18$) and faint ($b_J > 18$) galaxies excludes a luminosity segregation between the two groups at a confidence level of 30%. Also the spatial distribution on the plane of the sky does not present significant differences.

The luminosity function of A3556, which is reported in Figure 4b, is different from those of the other two clusters (see below), because it is rather flat for magnitudes brighter than ~ 16 , forming a “plateau”. This excess of bright galaxies is confirmed by the fact that the number of galaxies in A3556 with $b_J < 15.5$ is the same as in A3558 (6 objects within one Abell radius), but its total number is only 60% of the latter cluster. Considering only galaxies in the magnitude range $[15.5 - 19.5]$, we found $\alpha = -1.10_{-0.29}^{+0.32}$ and $M^* = -19.14_{-0.73}^{+0.50}$, with an effective (i.e. background subtracted) number of objects of 151. These values are significantly different from the “typical” parameters found for clusters: however, the observed luminosity function of this cluster could be a complex combination of two components (as suggested by the bimodality in the velocity distribution), whose single contributions are not easily separable.

Venturi et al. (1997) found that all the galaxies belonging to the plateau of the luminosity function are radio loud, suggesting a possible connection between the shape of the bright part of the luminosity function and the enhanced probability for a galaxy to have radio emission. Moreover, the presence of a remarkable low surface brightness extended radio source (dubbed J1324-3138 by Venturi et al. 1997) is revealed. It seems to be associated with a $b_J = 15.6$, $v = 15142$ km/s optical galaxy. Venturi et al. (1997) concluded that, given its steep spectrum, this source could be a narrow angle tail radio galaxy at the latest stage of its life. The fact that J1324-3138 belongs to the higher velocity group, which on the basis of the velocity dispersion could be considered the least massive component and thus falling toward the main component of A3556, suggests the presence of significant ram pressure acting on the radio source due to the interactions between intracluster media. This effect probably accounts for the evolution of radio sources in the diffuse emissions typically found in merging clusters (Ferretti & Giovannini 1996) and could be responsible for the properties of J1324-3138.

The galaxy density profile for this cluster is not well fitted by a King law. This fact is probably due to the different distribution of bright and faint galaxies, as shown in Figures 4c and 4d, where the profiles for galaxies with $b_J \leq 18$ and $b_J > 18$ are reported. The bright galaxies distribution appears quite centrally peaked, as confirmed by the parameters of the fit: we find $I_0 = 0.45$ arcmin⁻² (corresponding to 258 h² Mpc⁻²), $r_c = 0.90$ arcmin (0.04 h⁻¹ Mpc), $\alpha = 0.55$ and $bck = 0.01$ arcmin⁻² (7.5 h² Mpc⁻²). The fitted background is in good agreement with the value derived from the control area, in the same magnitude range ($bck = 0.011$ arcmin⁻²). On the contrary, the distribution of faint galaxies appears quite flat up to a radius of 15 arcmin, while it is consistent with the background density (dashed line in Figure 4d) for larger radii: this distribution is not well fitted with a simple King profile. For this reason, the parameters of the luminosity function given above were derived computing w_i following eq.(3) for $b_J \leq 18$ and eq.(5) for $b_J > 18$.

The complex behaviour of the density profile could be related to the presence of the two substructures found in the dynamical analysis: however, it is not possible to separate the contribution of these two components and therefore to properly estimate the cluster mass.

4.2 A3558

A3558, alias Shapley 8 or SC 1325–11, is a Bautz–Morgan type I cluster, classified by ACO in the richness class 4, and could be regarded as the dominant component of the cluster complex. In literature there is a large number of galaxy redshifts taken by Metcalfe et al. (1987), Teague et al. (1990), Stein (1996) and by us (Paper I). We estimated a mean velocity and a velocity dispersion of $\langle v \rangle = 14242 \pm 80$ km/s and $\sigma = 986 \pm 60$ km/s, within 1077 arcsec (corresponding to ~ 0.5 Abell radii) from the cluster center. In Paper I we showed that for larger distances the contamination by objects belonging to the nearby groups (SC 1327–312 and SC 1329–314) becomes not negligible.

In Paper II we studied a deep (~ 30 ksec) ROSAT PSPC X–ray observation of this cluster in the $[0.1 - 2.4]$ keV band. This cluster results to be rather cold ($KT = 3.25$ keV), with an X–ray total luminosity of 1.1×10^{44} h $^{-2}$ erg s $^{-1}$ in the $[0.5 - 2.0]$ keV band. The dynamical mass, estimated on the basis of the hydrostatic equilibrium, is 3.1×10^{14} h $^{-1}$ M $_{\odot}$ inside one Abell radius and results to be a factor 4 lower than the virial mass estimate of Metcalfe et al. (1994). Given the X–ray luminosity and the dynamical mass, it is clear that the optical richness of A3558 is overestimated (Paper II, Breen et al. 1994): Metcalfe et al. (1994) estimated a corrected richness class of 2. The explanation of this overestimate is probably the contamination due to nearby groups in this region.

Very recently, Markevitch & Vikhlinin (1997), studying a 17 ksec image of A3558 taken with the GIS detector of ASCA, estimated a temperature of 5.5 keV. On the basis of the gas temperature – velocity dispersion relation of Lubin & Bahcall (1993)

$$\sigma = 332 (KT)^{0.6} \quad (10)$$

the higher ASCA temperature appears to be more consistent with the galaxy velocity dispersion than the ROSAT one (which corresponds to $\sigma \sim 700$ km/s). On the other hand, Bird (1994) and Girardi et al. (1997), applying various tests for substructure detection, found that the velocity dispersion of A3558 is significantly affected by subclumps. After having corrected the sample for this effect, they determine a velocity dispersion of 781^{+178}_{-187} km/s and 735^{+49}_{-41} km/s, respectively.

The discrepancy between the two temperature values could indicate the existence of a calibration problem in one of the two satellites. However, this situation is very similar to the case of A2255 (Feretti et al. 1997), for which the ROSAT temperature (3.5 keV) is significantly lower than that obtained by Einstein (7.3 keV) in a slightly higher energy window, and of Hydra A (Ikebe et al. 1997), for which $T_{ROSAT} < T_{ASCA}$. The authors claim that this discrepancy could be the result of several co-existing components at different temperatures.

Adding the new redshift data to the catalogue, we estimate a global mean velocity of $\langle v \rangle = 14403^{+60}_{-55}$ km/s and a

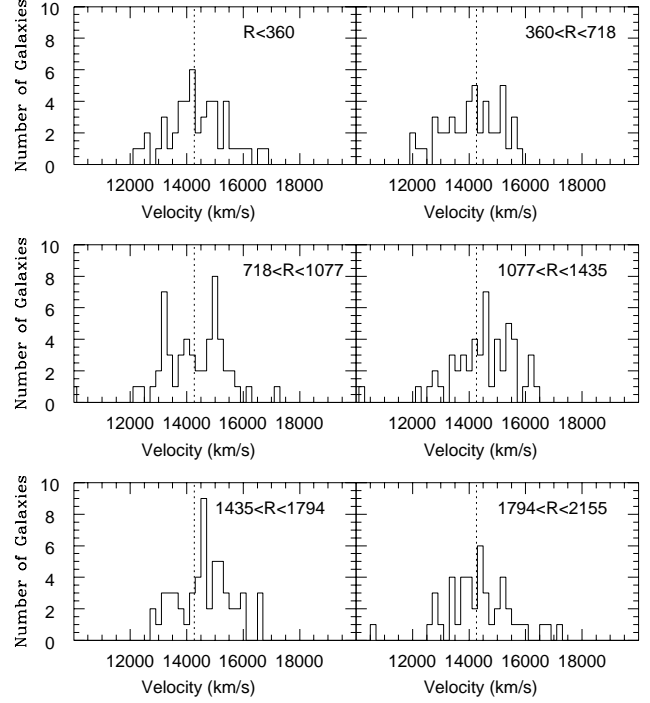


Figure 5. Redshift distribution of A3558 in various shells centered on the cluster center. In particular note, in the $[718 - 1077]$ arcsec shell, the presence of two peaks at $v \sim 13000$ km/s and $v \sim 15000$ km/s. The dashed line represents the mean velocity of 14262 km/s, determined within a region of ~ 0.5 Abell radii.

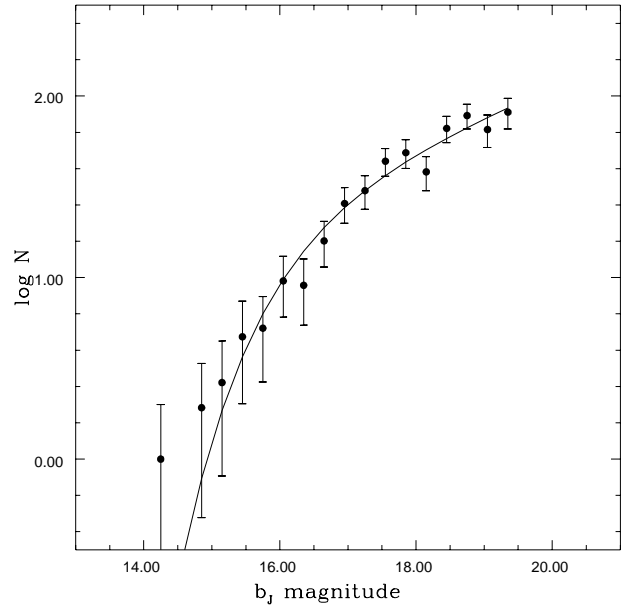


Figure 6. Luminosity function of A3558. The fitted parameters are $\alpha = -1.39^{+0.12}_{-0.12}$ and $M^* = -20.26^{+0.39}_{-0.56}$. The effective number of galaxies is 525.

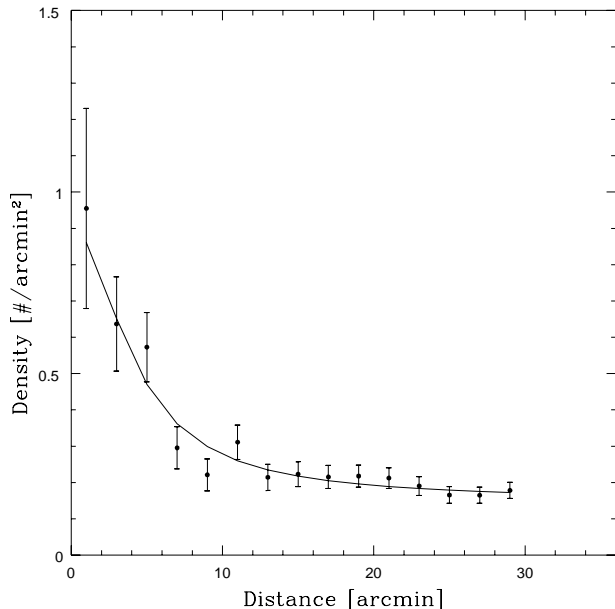


Figure 7. Galaxy density distribution in A3558, as a function of the distance from the cluster center. No background subtraction has been applied in this figure.

velocity dispersion of $\sigma = 996^{+40}_{-36}$ km/s within one Abell radius and using 307 galaxies. However, the considered region contains SC 1327–312 and its boundaries are very nearby to SC 1329–313 and A3556 and could be contaminated by galaxies of these clusters. For this reason, we restricted the analysis to 0.5 Abell radii finding $\langle v \rangle = 14262^{+75}_{-82}$ km/s and $\sigma = 992^{+85}_{-60}$, determined with 155 objects. Both these values are in agreement with those found in Paper I.

Metcalf et al. (1994), on the basis of 88 redshifts, found a difference in velocity dispersion between galaxies fainter and brighter than $m_B = 17$ and belonging to the “red sequence” characterizing the cluster. Using all galaxies within 0.5 Abell radii, without any selection in color, we find the same effect, but at a marginal (1.7 sigma) significance level. In fact, the 31 galaxies brighter than $b_J = 17$ have $\langle v \rangle = 14309^{+285}_{-219}$ km/s and $\sigma = 1125^{+139}_{-79}$ km/s, while the fainter ones (117 objects) have $\langle v \rangle = 14260^{+100}_{-67}$ km/s and $\sigma = 946^{+70}_{-80}$ km/s. At face value, this result is opposite to that of Biviano et al. (1992) who found, using a sample of 68 clusters, that the brightest members have a lower velocity dispersion with respect to the faintest ones. However, from the KMM analysis we find that the higher velocity dispersion of bright galaxies may be due to the superposition of two separate groups (homoscedastic bimodality significant at 96%). If we assume that the system is described by two Gaussians, the biweight means and velocity dispersions are $\langle v \rangle = 12993^{+129}_{-119}$ km/s and $\sigma = 310^{+119}_{-92}$ km/s ($N_{gal} = 11$) and $\langle v \rangle = 14871^{+144}_{-145}$ km/s and $\sigma = 455^{+51}_{-55}$ km/s ($N_{gal} = 20$). These two groups do not appear to be separated on the plane of the sky. We consider this bimodality, which can not be discussed further due to the small number of galaxies, only as an indication of the complex velocity distribution of bright galaxies in A3558.

The complicated dynamical state of the whole cluster is well illustrated by Figure 5, where we show the velocity

histograms in the six radial distance bins defined in Paper I. The dashed line is the mean velocity as estimated in the inner 1077 arcmin (14262 km/s). The dynamical parameters calculated in these velocity intervals are essentially the same as those of Table 5 in Paper I: the mean velocity is constant inside 0.5 Abell radii and increases in the three most external bins. In five out of six bins the velocity histograms are reasonably symmetric and featureless. The only exception is the third bin ($718 < R < 1077$ arcsec), where two peaks at 13200 and 15000 km/s are clearly visible. The bimodality is significant at the 98% level, giving $\langle v \rangle_1 = 13457^{+115}_{-114}$ km/s, $\sigma_1 = 470^{+88}_{-68}$ km/s and $\langle v \rangle_2 = 15011^{+77}_{-91}$ km/s, $\sigma_2 = 349^{+71}_{-59}$ km/s, with $N_1 = 25$ and $N_2 = 27$ galaxies, respectively. Note that the structure at higher velocity has parameters which are consistent within 1 sigma with the farther component of the distribution of the bright galaxies discussed above.

An analysis of the isodensity contours (see for example Figure 14b of Paper I), shows the presence of an excess of galaxies in this third shell, southern of the center of A3558. This substructure is revealed by the West et al. (1988) test, which measures the degree of symmetry of the bi-dimensional distribution with respect to the cluster center. Most of the galaxies in the lower velocity peak reside in this substructure: moreover, in this density excess there are two galaxies detected in the ROSAT X-ray band (#6 and #9 in Paper II) with $v = 13186$ km/s, $b_J = 15.1$, and $v = 12801$ km/s, $b_J = 15.8$, respectively.

In order to detect other substructures, we applied the Dressler & Shectman (1988) Δ test, which uses both positional and velocity information. These authors suggest a bootstrap procedure in order to estimate the presence of significant substructures in a cluster: following this procedure we found that A3558 shows evidence of substructures at more than 3σ level, and the most significant signal is due to a condensation centered at $\alpha(2000) \sim 13^h 29^m 16^s$ and $\delta(2000) \sim -31^\circ 18' 45''$, well in agreement with the position of the structure found by Girardi et al. (1997) and ~ 10 arcmin away from that found by Bird (1994). This substructure is in the quadrant of the cluster where Markevitch & Vikhlinin (1997), in their analysis of an ASCA X-ray map of A3558, found a significant increase of the hot gas temperature. The detailed analysis of the substructures in A3558 will be presented elsewhere (Bardelli et al., in preparation).

The parameters of the Schechter fit to the luminosity function are $\alpha = -1.39^{+0.12}_{-0.12}$ and $M^* = -20.26^{+0.39}_{-0.56}$, when galaxies within one Abell radius are considered (Figure 6). The effective number of objects belonging to the cluster is 525, i.e. 68% of the total. This result does not significantly change when considering a smaller radius. These values are in agreement with those found by Lumsden et al. (1997), who estimated an average luminosity function with $\alpha = -1.22 \pm 0.04$ and $M^* = -20.16 \pm 0.02$, using a sample of 22 clusters, obtained from the Edinburgh–Durham Southern Galaxy Catalogue (derived from COSMOS scans) and therefore directly comparable with our data. These values are also consistent with those found by Colless (1989) for 14 APM clusters ($\alpha = -1.21$ and $M^* = -20.04$). This agreement indicates that the magnitude distribution of galaxies in A3558 is not strongly modified by the interactions between this cluster and the nearby ones.

On the contrary, Metcalfe et al. (1994), on the basis

of scans of plates in the *B* band, found a flatter luminosity function ($\alpha = -1.0$, $M_B^* = -19.50$) for A3558. This discrepancy arises from the different galaxy counts in the two photometric samples, but its origin is unclear: it could be due to incompleteness of one of the two catalogues at faint magnitudes, or to systematic photometric errors, or to problems in the plate quality.

For what concerns the radial density profile, as already noted by Metcalfe et al. (1994), the parameters are poorly constrained. The minimum of the likelihood function is not well defined and this leads to very large uncertainties on the parameters. Our best estimates are $I_o = 0.90 \text{ arcmin}^{-2}$ (corresponding to $459 \text{ h}^2 \text{ Mpc}^{-2}$), $r_c = 3.6 \text{ arcmin}$ ($0.15 \text{ h}^{-1} \text{ Mpc}$), $\alpha = 0.85$ and $bck = 0.15 \text{ arcmin}^{-2}$ ($86 \text{ h}^2 \text{ Mpc}^{-2}$) (Figure 7). Note that the fitted background is a factor ~ 2 higher than the value derived from the control area ($bck = 0.076 \text{ arcmin}^{-2}$): this is probably due to the fact that A3558 is embedded in the center of a high density structure.

The comparison with the results of Metcalfe et al. (1994) is not straightforward, because I_o and bck depend on the different photometric band: moreover, their parameters were obtained by fixing the slope or the background. However, our slope and core radius are consistent at $\sim 10\%$ with those of case (1) for the red sequence galaxies of Metcalfe et al. (see their Table 4).

From the radial distribution of galaxies we estimated the mass of the cluster (eq.8): using a velocity dispersion of $\sigma = 992 \text{ km/s}$ we found $M(< 0.75 \text{ h}^{-1} \text{ Mpc}) = 4.5 \times 10^{14} \text{ h}^{-1} \text{ M}_\odot$ and $M(< 1.5 \text{ h}^{-1} \text{ Mpc}) = 9.2 \times 10^{14} \text{ h}^{-1} \text{ M}_\odot$, ~ 1.3 times lower than the estimates of Biviano et al. (1993) [$M(< 0.75 \text{ h}^{-1} \text{ Mpc}) = 6 \times 10^{14} \text{ h}^{-1} \text{ M}_\odot$] and Metcalfe et al. (1994) [$M(< 1.5 \text{ h}^{-1} \text{ Mpc}) = 1.2 \times 10^{15} \text{ h}^{-1} \text{ M}_\odot$], obtained applying the virial theorem. On the other hand Dantas et al. (1997), after having removed a substructure, estimated $M(< 0.75 \text{ h}^{-1} \text{ Mpc}) = 3.40 \times 10^{14} \text{ h}^{-1} \text{ M}_\odot$, under the hypothesis that galaxies orbit around a common central potential.

These differences can be a consequence of the different hypotheses on which the mass estimate methods are based (see e.g. the discussion in Bahcall & Tremaine 1981) and/or of the different choices for the cluster parameters, as f.i. the velocity dispersion. Our derived mass is factor ~ 3 or ~ 2 greater than the X-ray determination, using a gas temperature of 3.25 keV or 5.5 keV , respectively.

4.3 SC 1329–314

In Paper I, from the bi-dimensional and redshift distribution of galaxies between A3562 and A3558, we presented some evidence that the poor cluster SC 1329–314 can be considered as formed by two entities. In particular, some degree of luminosity segregation might be present between the two substructures. In Paper II, on the basis of the ROSAT observation of A3558, we confirmed the existence of both potential wells, revealing diffuse hot gas emission, as done also by Breen et al. (1994) using an Einstein observation.

Breen et al. (1994) dubbed the two groups SC 1329–313 and SC 1327–312 (named by us SC 1329–314A and SC 1329–314B in Paper I): for simplicity we will adopt their terminology. Although we do not have new redshift information for these systems, the detection of the diffuse gas

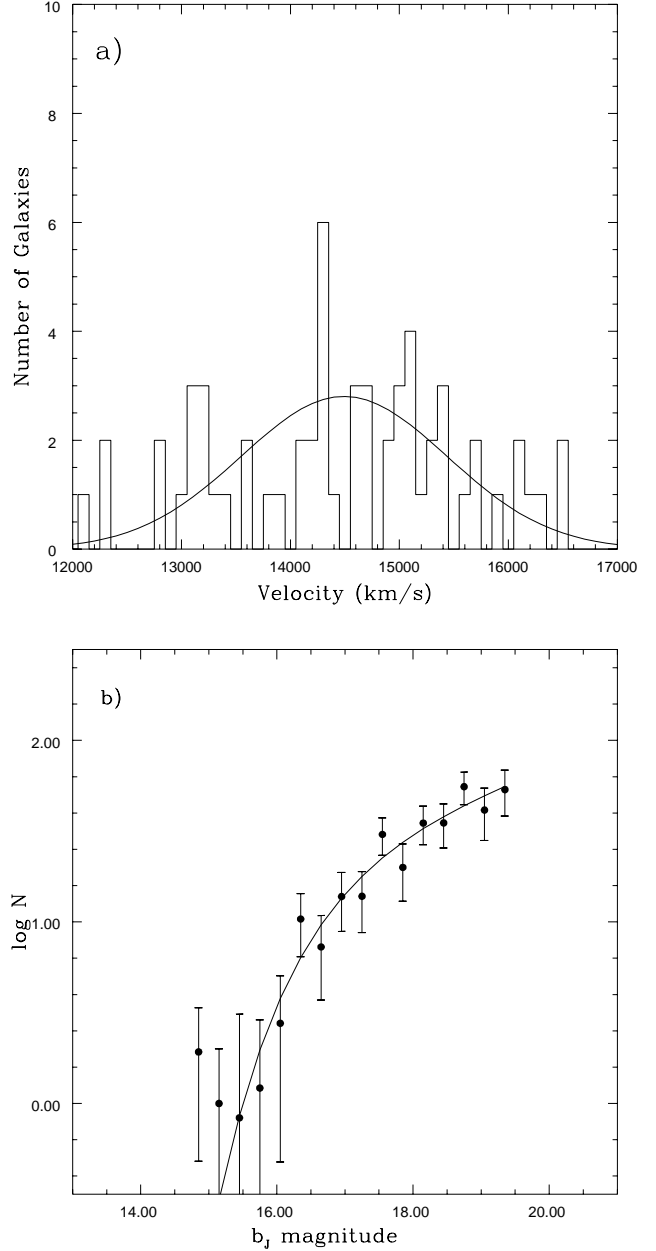


Figure 8. a) Redshift distribution of A3562. The Gaussian has parameters $\langle v \rangle = 14492^{+225}_{-286} \text{ km/s}$ and $\sigma = 913^{+189}_{-96} \text{ km/s}$, obtained from a sample of 21 galaxies within 10 arcmin from the cluster center.

b) Luminosity function of A3562. The fitted parameters are $\alpha = -1.42^{+0.19}_{-0.15}$ and $M^* = -19.84^{+0.46}_{-0.61}$.

can help us to better define the centers and sizes of these groups, avoiding (or at least decreasing) the possibility of contamination from the overall complex. We decided to use the positions obtained from the X-ray frame in which the groups are better centered: therefore for SC 1329–313 the coordinates given by Breen et al. [$\alpha(2000) = 13^{\text{h}}31^{\text{m}}36^{\text{s}}$ and $\delta(2000) = -31^{\circ}48'46''$] are assumed, while for SC 1327–312 we prefer the center given in Paper II [$\alpha(2000) = 13^{\text{h}}29^{\text{m}}47^{\text{s}}$ and $\delta(2000) = -31^{\circ}36'29''$]. For each group we selected all galaxies within 10 arcmin from the center.

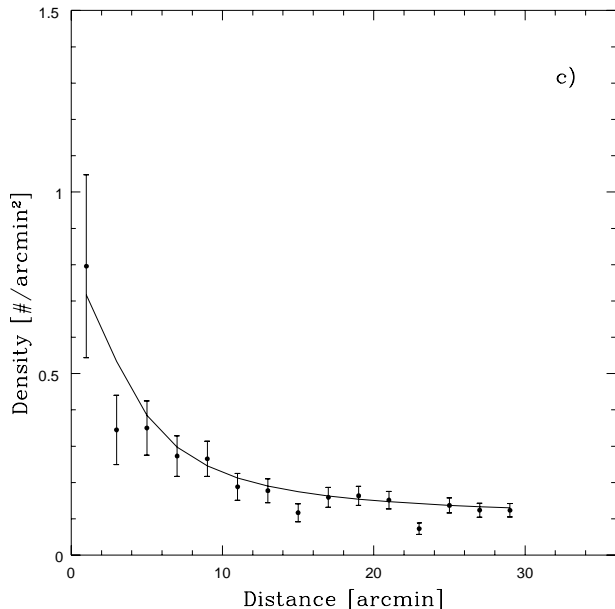


Figure 8. c) Galaxy density distribution in A3562, as a function of the distance from the cluster center. No background subtraction has been applied in this figure.

The clump SC 1329–313 is more evident as bi-dimensional overdensity (see Figure 14 of Paper I). The velocity histogram of the sample obtained with the X-ray center shows bimodality, confirmed by the KMM test at 97% confidence level. The two distributions have $\langle v \rangle = 14790^{+114}_{-67}$ km/s, $\sigma = 377^{+93}_{-82}$ km/s and $\langle v \rangle = 13348^{+69}_{-83}$ km/s, $\sigma = 276^{+70}_{-61}$ km/s; the number of objects used is 16 and 21, respectively. Note that the use of the X-ray position to select galaxies leads to a more reasonable determination of the velocity dispersion, with respect to the former value of ~ 900 km/s given in Paper I, which evidently was contaminated by galaxies belonging to the overall structure, hiding the bimodality.

The subcondensation SC 1327–312 appears to be connected to A3558 by a significant bridge of hot gas, signature of strong mareal interactions, and it is possible that the connection is extending also to A3562. SC 1327–312, although less evident in the optical isodensity contours, has an X-ray luminosity that is a factor ~ 2.5 greater than that of SC 1329–313 and only a half of that of A3562 (see Table 2 of Breen et al. 1994). With 24 redshifts we obtained $\langle v \rangle = 14844^{+195}_{-211}$ and $\sigma = 691^{+158}_{-146}$; the X-ray temperature extrapolated from eq.(10) is 3.4 keV, in agreement with that found by Breen et al. (1994).

4.4 A3562

A3562 is a Bautz–Morgan type I cluster, with richness class 2. Previous determinations of the mean velocity and velocity dispersion are $\langle v \rangle = 14724 \pm 232$ km/s and $\sigma = 825^{+213}_{-120}$ km/s from Quintana et al. (1995), based on 15 redshifts. David et al. (1993) reported a hot gas temperature of $KT = 3.8 \pm 0.5$ keV from an EXOSAT observation. The spectroscopic sample for this cluster is rather small and the dynamical situation complex: the existence of a “finger-of-God” effect for the

cluster is not clear and there can be a contamination from a filamentary structure extending from ~ 12000 to ~ 14000 km/s in the East–West direction (see Figure 2). Moreover, there could be also a contamination from SC 1329–313. For these reasons we restricted the sample to a region with radius smaller than 10 arcmin from the center in the analysis of the dynamical parameters: we find $\langle v \rangle = 14492^{+225}_{-286}$ km/s and $\sigma = 913^{+189}_{-96}$ km/s with 21 galaxies, in agreement with the Quintana et al. (1995) results. In Figure 8a we show the velocity distribution of all galaxies within one Abell radius from the center of A3562; the superimposed Gaussian has the parameters reported above.

The velocity dispersion is consistent, within the errors, with the reported X-ray temperature: however, the small number of redshifts used prevent us from a more detailed analysis and we can not exclude a more complicated scenario for this cluster, due to contaminations from nearby groups or to the presence of substructures.

The parameters of the luminosity function reported in Figure 8b are $\alpha = -1.42^{+0.19}_{-0.15}$ and $M^* = -19.84^{+0.46}_{-0.61}$, with an effective number of galaxies of 322. The α and M^* values are consistent with those of A3558, indicating a similar population of galaxies.

The radial surface density of galaxies has been fitted and the derived parameters are $I_o = 0.70$ arcmin $^{-2}$ (corresponding to 401 h 2 Mpc $^{-2}$), $r_c = 3.1$ arcmin (0.13 h $^{-1}$ Mpc), $\alpha = 0.70$ and $bck = 0.10$ arcmin $^{-2}$ (57 h 2 Mpc $^{-2}$) (Figure 8c). The fitted background is $\sim 30\%$ higher than the value obtained from the control area. The corresponding mass is $M(< 0.75$ h $^{-1}$ Mpc) = 3.4×10^{14} h $^{-1}$ M $_{\odot}$ and $M(< 1.5$ h $^{-1}$ Mpc) = 7.0×10^{14} h $^{-1}$ M $_{\odot}$.

5 SUMMARY

In this paper we have presented 174 new galaxy redshift determinations in the direction of the core of the Shapley Concentration, a complex formed by the three ACO clusters A3558, A3556 and A3562. These velocities are added to the previous samples of Paper I and of Quintana et al. (1995) obtaining a final list of 714 velocities. The percentage of galaxies presenting emission lines is 17%, consistent with that found in other clusters. This new sample confirms the early claim that this structure is formed by strongly interacting clusters and is elongated (for ~ 7.5 h $^{-1}$ Mpc) perpendicular to the line of sight.

With this larger sample, we found that this structure is characterized by a large number of subcondensations: A3556, A3558 and SC 1329–313 appear to have subclumps. In particular, we detected a group with $\sigma = 222$ km/s which is probably infalling toward the main component of A3556 and which hosts the extended radio source J1324–3138 described in Venturi et al. (1997). The interaction between the media of the two clumps could be responsible of the ram pressure acting on the source.

Applying the substructure test of Dressler & Shectman (1988) we found a significant clump in A3558, in the cluster quadrant with higher X-ray temperature (Markevitch & Vikhlinin 1997). Moreover, the two elliptical galaxies detected as X-ray sources in the ROSAT map of A3558 (see Paper II) are found to reside in a small group southward

with respect to the center of the cluster, at a distance of ~ 18 arcmin.

For the three ACO clusters of the complex we derived the luminosity functions, adopting a new fitting technique which takes into account the galaxy density profiles. The dynamical complexity of this region does not seem to influence noticeably the magnitude and density distributions of A3558 and A3562, which are similar to other clusters. The luminosity function of A3556 has a remarkably fainter cut off with respect to the “mean” Schechter function of clusters as estimated by Colless (1989) and Lumsden et al. (1997) and appears to have a “plateau” for magnitude brighter than $b_J=15.5$: the corresponding galaxies are all radio emitters. Moreover, from the density profile, galaxies fainter than $b_J = 18$ appear to have a flatter radial distribution while the brighter objects are more concentrated toward the cluster center.

The core of the Shapley Concentration, a single connected structure embedding three cluster cores and other minor subcondensations, resembles the result of the detailed simulations performed by McGlynn & Fabian (1984) and Roettiger et al. (1993), who studied cluster–cluster and cluster–group merging, respectively.

Our general conclusion is that the central part of the Shapley Concentration is an active region for what concerns dynamical interactions, where rich clusters are forming through a bottom–up hierarchical process. In particular, the A3558 cluster complex could be a cluster–cluster collision seen just after the first core–core encounter, where an intervening cluster impacted onto the richer object A3558. Indeed, the clumpiness found eastward of A3558 could be due to the galaxies of this intervening cluster, which is now emerging from the main component. However, this major merging event does not seem to have modified substantially the galaxy luminosity distribution in the richer components A3558 and A3562. This implies that, at least during the early stages of this phenomenon, the galaxy–galaxy interactions are not very important.

This scenario is not unexpected in a rich environment such as the central part of a supercluster, where peculiar velocities of the order of ~ 1000 km/s are expected. In particular, another similar structure is found ~ 10 degrees westward of the A3558 complex, dominated by the three ACO clusters A3528, A3530 and A3532. The analysis of a redshift survey toward these objects is in progress. Moreover, in order to determine the galaxy overdensity of the inner $10 h^{-1}$ Mpc, we performed a redshift survey of galaxies between clusters: the results of these analyses will be presented elsewhere (Bardelli et al., in preparation).

ACKNOWLEDGEMENTS

We warmly thank Luca Ciotti for helpful discussions. This work has been partially supported through the ASI Contract 95–RS–152. We thank the referee for useful comments.

REFERENCES

- Abell, G.O., Corwin Jr., H.G., Olowin, R.P., 1989, *ApJSS* 70, 1 [ACO catalogue]
- Allen, D.A., Norris, R.P., Staveley–Smith, L., Meadows, V.S., Roche, P.F., 90, *Nat* 343, 45.
- Ashman, K.M., Bird, C.M., Zepf, S.E., 1994, *AJ* 108, 2348
- Bahcall, J.N., Tremaine, S., 1981, *ApJ* 244, 805
- Bardelli, S., Zucca, E., Vettolani, G., Zamorani, G., Scaramella, R., Collins, C.A., MacGillivray, H.T., 1994, *MNRAS* 267, 665 [Paper I]
- Bardelli, S., Zucca, E., Malizia, A., Zamorani, G., Scaramella, R., Vettolani, G., 1996, *A&A* 305, 435 [Paper II]
- Bardelli, S., Zucca, E., Vettolani, G., Zamorani, G., Scaramella, R., 1997, *Proceedings of Observational Cosmology: from Galaxies to Galaxy Systems, Astroph. Letters and Comm., in press*
- Beers, T.C., Flynn, K., Gebhardt, K., 1990, *AJ* 100, 32
- Binney, J., Tremaine, S., 1987, *Galactic Dynamics*, Princeton University press, Princeton, p.205
- Bird, C.M., Beers, T.C., 1993, *AJ* 105, 1596
- Bird, C.M., 1994, *AJ* 107, 1637
- Biviano, A., Girardi, M., Giuricin, G., Mardirossian, F., Mezzetti, M., 1992, *ApJ* 396, 35
- Biviano, A., Girardi, M., Giuricin, G., Mardirossian, F., Mezzetti, M., 1993, *ApJ* 411, L13
- Biviano, A., Katgert, P., Mazure, A., Moles, M., den Hartog, R., Focardi, P., 1997a, *Proceedings of Observational Cosmology: from Galaxies to Galaxy Systems, Astroph. Letters and Comm., in press*
- Biviano, A., Katgert, P., Mazure, A., Moles, M., den Hartog, R., Perea, J., Focardi, P., 1997b, *A&A* 321, 84
- Branchini, E., Plionis, M., 1996, *ApJ* 460, 569
- Breen, J., Raychaudhury, S., Forman, W., Jones, C., 1994, *ApJ* 424, 59
- Briel, U.G., Henry, J.P., Schwarz, R.A., Böhringer, H., Ebeling, H., Edge, A.C., Hartner, G.D., Schindler, S., Trümper, J., Voges, W., 1991, *A&A* 246, L10
- Burns, J.O., Roettiger, K., Ledlow, M., Klypin, A., 1994, *ApJ* 427, L90
- Burstein, D., Heiles, C., 1984, *ApJSS* 54, 33
- Colless, M., 1989, *MNRAS* 237, 799
- Danese, L., De Zotti, G., di Tullio, G., 1980, *A&A* 82, 322
- Dantas, C.C., de Carvalho, R.R., Capelato, H.V., Mazure, A., 1997, *ApJ* 485, 447
- David, L.P., Slyz, A., Jones, C., Forman, W., Vrtilik, S.D., Arnaud, K.A., 1993, *ApJ* 412, 479
- Dressler, A., Shectman, S.A., 1988, *AJ* 95, 985
- Feretti, L., Böhringer, H., Giovannini, G., Neumann, D., 1997, *A&A* 317, 432
- Feretti, L., Giovannini, G., 1996, in *Extragalactic Radio Sources*, IAU Symposium 175, Ekers, R., Fanti, C., Padrielli, L. eds., Kluwer academic publ., Dordrecht, p.334
- Girardi, M., Biviano, A., Giuricin, G., Mardirossian, F., Mezzetti, M., 1995, *ApJ* 438, 527
- Girardi, M., Escalera, E., Fadda, D., Giuricin, G., Mardirossian, F., Mezzetti, M., 1997, *ApJ* 482, 41
- Heydon–Dumbleton, N.H., Collins, C.A., MacGillivray, H.T., 1989, *MNRAS* 238, 379
- Kurtz, M.J., Mink, D.J., Wyatt, W.F., Fabricant, D.G., Torres, G., Kriss, G.A., Tonry, J.L., 1992, in *Astronomical Data Analysis Software and Systems I*, Worrall, D.M., Biemesderfer, C., and Barnes, J., eds., ASP conference series vol.25, p.432.
- Ikebe, Y., Makishima, K., Ezawa, H., et al., 1997, *ApJ* 481, 660
- Lahav, O., Edge, A.C., Fabian, A.C., Putney, A., 1989, *MNRAS* 238, 881
- Lubin, L.M., Bahcall, N.A., 1993, *ApJ* 415, L17
- Lumsden, S.L., Collins, C.A., Nichol, R.C., Eke, V.R., Guzzo, L., 1997, *MNRAS* in press (preprint astro-ph/9705120)
- Lund, G., 1986, *OPTOPUS - ESO operating manual N.6*
- Malumuth, E.M., Kriss, G.A., Van Dyke Dixon, W., Ferguson, H.C., Ritchie, C., 1992, *AJ* 104, 495

Markevitch, M., Vikhlinin, A., 1997, ApJ 474, 84
 McGlynn, T.A., Fabian, A.C., 1984, MNRAS 208, 709
 Metcalfe, N., Godwin, J.G., Spenser, S.D., 1987, MNRAS 225, 581
 Metcalfe, N., Godwin, J.G., Peach, J.V., 1994, MNRAS 267, 431
 Quintana, H., Ramirez, A., Melnick, J., Raychaudhury, S., Szelak, E., 1995, AJ 110, 463
 Raychaudhury, S., Fabian, A.C., Edge, A.C., Jones, C., Forman, W., 1991, MNRAS 248, 101
 Roettiger, K., Burns, J.O., Loken, C., 1993, ApJ 407, L53
 Scaramella, R., Baiesi-Pillastrini, G., Chincarini, G., Vettolani, G., Zamorani, G., 1989, Nature 338, 562
 Schechter, P., 1976, ApJ 203, 297
 Shapley, H., 1930, Bull. Harvard Obs. 874, 9
 Stein, P., 1996, A&ASS 116, 203
 Stein, P., 1997, A&A 317, 670
 Teague, P.F., Carter, D., Gray, P.M., 1990, ApJSS 72, 715
 The L.S., White, S.D.M., 1986, AJ 92, 1248
 Tremaine, S., in Dynamics and Interactions of Galaxies, 1990, Wielen, R., ed., Springer Verlag, Berlin, p.394
 Venturi, T., Bardelli, S., Morganti, R., Hunstead, R.W., 1997, MNRAS 285, 898
 West, M.J., Oemler, A., Dekel, A., 1988, ApJ 327, 1
 Wyse, R.F., Gilmore G., 1992, MNRAS 257, 1
 Yentis, D.J., et al., 1992, in Digitized Optical Sky Surveys, MacGillivray, H.T., Collins, C.A., eds., Kluwer, Dodrecht, p.67
 Zucca, E., Zamorani, G., Scaramella, R., Vettolani, G., 1993, ApJ 407, 470
 Zucca, E., Pozzetti, L., Zamorani, G., 1994 MNRAS 269, 953

Table 2. Redshift data

FIELD 1: α (2000) = 13 ^h 33 ^m 30 ^s δ (2000) = -31° 40' 00"						
#	α (2000)	δ (2000)	b_J	v	err	notes
1	13 33 58.02	-31 29 24.9	14.85	10876	77	
2	13 33 49.97	-31 43 15.8	16.24	16162	50	
3	13 34 23.16	-31 44 07.5	16.33	16311	50	
4	13 34 35.87	-31 41 07.0	16.48	11357	89	
5	13 33 50.37	-31 28 39.2	16.59	10994	12	emiss
6	13 33 42.03	-31 32 37.1	16.75	15379	59	
7	13 33 37.54	-31 33 18.3	16.76	14289	53	
8	13 33 17.22	-31 29 33.6	16.88	14336	64	
9	13 32 46.44	-31 37 03.4	16.88	12317	8	emiss
10	13 33 47.86	-31 33 22.2	16.97	13067	44	
11	13 32 39.21	-31 49 52.6	17.14	12797	51	
12	13 33 11.67	-31 40 09.8	17.25	14269	74	
13	13 32 35.24	-31 31 46.2	17.28	15193	18	emiss
14	13 32 43.87	-31 47 01.7	17.33	12836	36	emiss
15	13 33 31.93	-31 36 40.6	17.33	15716	87	
16	13 33 37.07	-31 38 29.9	17.36	14995	43	
17	13 34 07.19	-31 29 22.0	17.39	15288	77	
18	13 33 41.03	-31 42 52.4	17.46	13610	64	
19	13 34 38.49	-31 40 19.2	17.56	13154	71	
20	13 34 30.43	-31 36 50.2	17.59	14567	83	
21	13 33 09.49	-31 36 12.8	17.60	14557	65	
22	13 33 13.25	-31 34 13.3	17.64	13382	87	
23	13 32 28.80	-31 36 52.4	17.67	15044	87	
24	13 34 02.55	-31 37 00.8	17.70	14152	157	
25	13 33 23.42	-31 29 02.1	17.78	13049	53	emiss
26	13 32 37.37	-31 44 24.3	17.99	15444	33	emiss
27	13 34 43.36	-31 40 23.0	18.02	10391	3	emiss
28	13 33 16.51	-31 43 41.7	18.13	22007	28	emiss
29	13 33 59.61	-31 47 05.7	18.32	13110	88	
30	13 33 04.08	-31 39 04.6	18.32	14120	7	emiss
31	13 34 01.63	-31 26 08.5	18.33	14683	93	
32	13 34 08.11	-31 47 35.5	18.34	15335	154	
33	13 33 08.46	-31 29 39.0	18.43	14256	70	
34	13 32 51.80	-31 34 40.9	18.45	15674	52	
35	13 32 39.43	-31 48 36.7	18.56	14421	61	
36	13 32 22.23	-31 44 18.7	18.61	12340	20	emiss
37	13 33 32.91	-31 31 18.7	18.73	15092	135	
38	13 33 16.84	-31 25 48.3	18.79	13757	31	emiss
39	13 33 22.67	-31 33 10.0	18.80	16122	80	
40	13 32 43.98	-31 48 35.6	18.83	14303	82	

Table 2. cont.

FIELD 2: α (2000) = 13 ^h 23 ^m 36 ^s δ (2000) = -31° 39' 21"						
#	α (2000)	δ (2000)	b_J	v	err	notes
1	13 24 18.66	-31 50 33.5	17.49	16138	41	
2	13 23 43.86	-31 47 01.8	17.67	14325	71	
3	13 22 42.52	-31 32 33.2	17.82	star		
4	13 24 46.36	-31 44 46.3	17.99	15437	72	
5	13 23 49.22	-31 42 57.5	18.04	12998	59	
6	13 24 06.62	-31 41 14.0	18.17	14952	50	
7	13 23 34.48	-31 47 19.6	18.30	14001	27	
8	13 23 41.72	-31 28 35.0	18.33	star		
9	13 22 32.96	-31 32 45.7	18.52	14147	95	
10	13 24 02.96	-31 49 45.5	18.54	13755	29	
11	13 23 06.47	-31 37 07.3	18.62	star		
12	13 24 31.96	-31 41 15.7	18.66	14117	37	
13	13 24 04.91	-31 47 47.5	18.67	15125	34	
14	13 24 40.30	-31 38 42.2	18.71	14296	35	
15	13 23 35.43	-31 52 01.2	18.72	14900	34	
16	13 23 17.04	-31 46 16.5	18.79	star		
17	13 24 10.75	-31 40 03.8	18.81	star		
18	13 23 04.76	-31 31 43.9	18.82	27265	95	
19	13 24 36.28	-31 47 41.1	18.83	35322	64	
20	13 23 48.15	-31 49 54.0	18.86	15074	27	
21	13 22 39.07	-31 48 01.5	18.87	star		
22	13 24 11.26	-31 30 57.6	18.89	13387	41	
23	13 23 10.74	-31 50 11.5	18.89	14019	31	
24	13 23 54.55	-31 37 21.1	18.90	55144	76	
25	13 23 50.14	-31 35 19.9	18.91	13986	28	
26	13 24 43.04	-31 32 39.4	18.93	13919	32	
27	13 22 36.07	-31 34 13.4	18.94	star		
28	13 23 44.51	-31 30 31.7	18.97	12864	64	
29	13 22 40.55	-31 40 24.5	18.98	star		
30	13 23 38.16	-31 40 52.5	18.99	star		
31	13 22 46.65	-31 44 03.1	19.00	14381	65	
32	13 24 17.69	-31 29 21.9	19.00	star		
33	13 23 40.96	-31 41 56.5	19.02	16443	39	emiss
34	13 24 37.17	-31 44 21.3	19.03	13967	85	
35	13 23 35.83	-31 53 29.0	19.04	star		
36	13 22 56.94	-31 38 54.8	19.04	star		
37	13 23 25.43	-31 32 48.1	19.06	40320	43	
38	13 24 25.97	-31 42 16.1	19.08	star		
39	13 23 19.77	-31 24 18.0	19.08	16480	4	emiss
40	13 23 07.65	-31 39 15.1	19.09	49858	79	
41	13 24 24.95	-31 49 49.4	19.11	star		
42	13 23 30.73	-31 34 38.7	19.12	star		
43	13 24 42.09	-31 32 01.6	19.13	14339	38	

Table 2. cont.

FIELD 3: α (2000) = 13 ^h 29 ^m 45 ^s δ (2000) = -32° 07' 43"						
#	α (2000)	δ (2000)	b_J	v	err	notes
1	13 30 03.99	-32 02 10.2	15.57	4537	20	emiss
2	13 29 55.95	-32 08 31.4	15.72	3873	63	
3	13 29 16.93	-32 02 35.0	16.15	13834	29	
4	13 30 34.64	-32 15 52.3	16.22	4027	33	
5	13 30 20.46	-32 05 50.1	16.26	12770	34	
6	13 30 52.08	-32 08 56.3	16.55	12932	31	
7	13 28 50.84	-32 07 54.3	16.86	15073	57	
8	13 30 21.19	-31 55 44.0	16.92	14204	28	
9	13 29 10.37	-32 05 24.3	17.10	13816	49	
10	13 30 36.42	-32 18 37.8	17.12	13040	26	
11	13 29 54.10	-32 01 00.5	17.25	14012	23	
12	13 30 06.42	-31 56 26.9	17.31	star		
13	13 30 18.90	-32 01 54.5	17.33	12927	39	
14	13 30 40.67	-32 05 35.6	17.36	12961	47	
15	13 29 01.36	-32 01 41.7	17.43	14047	52	
16	13 30 47.52	-32 02 36.7	17.44	13435	28	
17	13 30 07.95	-32 22 41.4	17.44	14618	31	
18	13 30 38.67	-32 03 28.9	17.51	13100	27	
19	13 28 51.47	-32 04 18.2	17.65	13479	28	
20	13 29 58.21	-32 12 27.1	17.68	14060	28	
21	13 28 41.84	-32 16 26.9	17.72	13779	45	
22	13 30 12.67	-32 07 24.2	17.73	14027	25	
23	13 29 33.66	-31 53 26.6	17.79	14525	14	emiss
24	13 28 58.74	-32 03 52.8	17.82	14467	20	
25	13 29 21.63	-31 59 35.7	17.85	star		
26	13 30 01.71	-31 56 49.4	17.99	14122	32	
27	13 28 46.44	-32 10 01.5	18.03	13710	11	emiss
28	13 30 02.02	-32 15 19.7	18.06	14936	36	
29	13 30 15.46	-32 03 59.7	18.07	13835	31	
30	13 30 02.85	-31 56 25.4	18.13	14855	37	
31	13 29 36.89	-32 20 47.9	18.34	star		
32	13 30 00.67	-32 18 33.1	18.46	12288	9	emiss
33	13 29 16.02	-32 16 37.7	18.49	38646	47	
34	13 29 49.34	-32 22 16.8	18.49	52895	49	
35	13 30 51.61	-32 11 43.6	18.54	12958	81	
36	13 29 06.33	-31 56 37.5	18.60	12705	8	emiss
37	13 30 29.12	-32 00 47.8	18.70	12884	68	
38	13 28 54.26	-31 56 25.3	18.70	15473	33	
39	13 29 37.35	-31 55 57.9	18.72	14238	81	
40	13 30 00.49	-31 52 28.6	18.73	13430	18	emiss
41	13 30 29.40	-32 13 53.2	18.80	4043	185	
42	13 28 53.62	-32 17 27.7	18.81	43458	28	

Table 2. cont.

FIELD 4: α (2000) = $13^h 27^m 15^s$ δ (2000) = $-32^\circ 05' 00''$						
#	α (2000)	δ (2000)	b_J	v	err	notes
1	13 26 55.63	-31 58 13.9	15.68	8058	74	
2	13 26 48.59	-31 59 47.1	15.75	14779	46	
3	13 26 52.72	-32 00 31.3	16.19	14004	40	
4	13 27 24.31	-32 18 01.4	16.34	14329	78	
5	13 27 06.52	-31 51 40.4	16.38	15407	33	
6	13 26 57.42	-32 11 53.8	16.57	13982	86	
7	13 27 15.64	-32 17 10.0	16.61	13057	58	
8	13 28 08.01	-32 08 48.4	16.69	21550	82	
9	13 27 12.92	-31 55 54.0	16.73	14623	41	
10	13 26 57.53	-31 56 07.6	17.25	14662	34	
11	13 27 03.20	-31 52 23.9	17.52	14947	34	
12	13 26 33.73	-31 56 56.1	17.52	15217	101	
13	13 27 51.39	-31 57 00.5	17.59	15152	33	
14	13 27 19.84	-31 54 50.8	17.66	13619	43	
15	13 27 18.62	-31 51 09.5	17.90	15568	54	
16	13 26 53.38	-31 52 26.1	17.94	14547	30	
17	13 26 26.65	-31 55 32.9	17.98	14911	81	
18	13 27 14.00	-31 59 15.5	18.02	14575	62	
19	13 26 58.45	-32 14 54.4	18.17	16589	51	
20	13 27 07.35	-32 00 12.6	18.19	15904	64	
21	13 27 36.20	-32 03 03.5	18.39	star		
22	13 26 59.92	-31 57 54.8	18.41	12843	104	
23	13 28 10.82	-32 12 52.6	18.44	43169	33	
24	13 27 49.44	-31 59 40.8	18.49	13553	27	
25	13 27 03.48	-32 16 26.4	18.49	16425	30	
26	13 27 09.48	-32 09 18.7	18.52	13791	88	
27	13 26 49.74	-31 51 24.8	18.58	star		
28	13 28 23.33	-32 06 55.4	18.66	21934	72	
29	13 27 10.94	-31 54 13.8	18.67	13140	50	
30	13 26 54.83	-31 59 49.3	18.67	14569	77	
31	13 27 14.63	-31 53 43.0	18.68	7959	10	emiss
32	13 28 16.84	-32 12 09.5	18.68	13134	36	
33	13 28 14.71	-32 08 30.1	18.70	star		
34	13 28 14.14	-32 12 33.2	18.72	star		
35	13 28 07.50	-32 14 43.7	18.75	43613	43	
36	13 27 32.96	-32 11 36.4	18.81	14474	94	
37	13 27 19.38	-31 54 14.3	18.81	37199	15	emiss
38	13 28 01.22	-32 04 34.6	18.85	14454	48	
39	13 26 45.57	-32 14 19.0	18.85	star		
40	13 26 17.24	-32 09 22.3	18.92	14344	59	
41	13 26 27.61	-31 53 43.8	18.97	58296	32	
42	13 26 48.09	-32 18 21.8	18.98	43351	42	
43	13 27 45.88	-31 51 17.5	19.00	14562	9	emiss
44	13 27 20.39	-32 12 15.8	19.02	13359	56	

Table 2. cont.

FIELD 5: α (2000) = $13^h 32^m 15^s$ δ (2000) = $-32^\circ 12' 17''$						
#	α (2000)	δ (2000)	b_J	v	err	notes
1	13 31 19.38	-31 13 45.0	16.35	15710	27	
2	13 31 06.07	-31 16 57.7	16.92	3958	10	emiss
3	13 31 14.90	-31 11 53.8	16.99	15607	35	
4	13 31 13.73	-31 13 02.4	17.01	14239	28	
5	13 32 09.09	-31 03 27.0	17.07	15729	38	
6	13 32 28.46	-31 03 50.1	17.17	13852	31	
7	13 31 47.71	-31 25 39.6	17.20	14214	32	
8	13 33 00.93	-31 13 29.6	17.53	11028	10	emiss
9	13 31 13.75	-31 16 28.3	17.68	13105	26	
10	13 31 22.32	-31 22 10.5	17.70	14027	13	emiss
11	13 32 11.64	-31 02 21.2	17.70	13425	30	
12	13 32 30.00	-31 03 16.6	17.74	13772	48	
13	13 33 20.34	-31 15 17.0	17.78	50004	54	
14	13 31 55.90	-31 14 19.6	17.82	13717	29	
15	13 32 55.16	-31 18 13.8	17.87	star		
16	13 32 05.32	-31 12 29.4	17.90	star		
17	13 32 31.63	-31 07 27.1	18.02	star		
18	13 31 42.47	-31 17 57.7	18.09	14056	11	emiss
19	13 31 55.52	-31 01 43.2	18.24	15235	29	
20	13 32 12.91	-31 12 44.7	18.30	star		
21	13 32 38.22	-31 01 41.8	18.32	13189	4	emiss
22	13 31 35.61	-31 23 28.2	18.32	star		
23	13 31 05.56	-31 12 57.7	18.33	star		
24	13 32 33.41	-31 20 51.0	18.33	star		
25	13 32 09.41	-31 09 24.3	18.35	star		
26	13 33 21.74	-31 05 12.2	18.36	33108	33	
27	13 31 19.20	-31 01 43.7	18.45	39256	90	
28	13 32 29.30	-31 06 18.7	18.48	30796	58	
29	13 32 36.01	-31 08 39.4	18.48	star		
30	13 32 28.11	-31 25 37.7	18.49	27119	108	
31	13 33 27.82	-31 12 54.2	18.53	13059	13	emiss
32	13 31 42.01	-31 10 43.3	18.57	star		
33	13 32 20.37	-31 12 01.3	18.63	star		
34	13 32 30.78	-31 02 07.8	18.66	13334	11	emiss
35	13 32 43.80	-31 23 09.0	18.66	star		
36	13 32 25.83	-31 20 17.1	18.71	14919	39	
37	13 32 52.33	-31 20 31.3	18.76	16546	35	
38	13 33 12.04	-31 08 19.1	18.80	star		
39	13 31 01.76	-31 10 49.1	18.80	star		
40	13 32 15.09	-31 13 29.8	18.81	44703	74	
41	13 31 54.07	-31 01 04.6	18.81	star		
42	13 31 53.30	-31 21 46.1	18.88	star		
43	13 31 22.88	-31 06 19.0	18.90	14483	53	
44	13 33 09.95	-31 22 42.2	18.93	star		
45	13 31 56.36	-31 08 53.2	18.94	15316	5	emiss